Long-term postoperative perfusion status in giant retinal tears: a case report

MIGUEL A. QUIROZ-REYES (drquiroz@prodigy.net.mx)
RETINA SPECIALISTS UNIT AT OFTALMOLOGIA INTEGRAL ABC https://orcid.org/0000-0001-7818-1911
ERICK A QUIROZ-GONZALEZ
INSTITUTE OF OPHTHALMOLOGY
MIGUEL A. QUIROZ-GONZALEZ
RETINA SPECIALISTS UNIT AT OFTALMOLOGIA INTEGRAL ABC
AHMADAD R. ALSABER
University of Strathclyde, Glasgow, UK
VIRGILIO LIMA-GOMEZ
HOSPITAL JUAREZ. MEXICO

Case Report

Keywords: deep vascular plexus, giant retinal tears, rhegmatogenous retinal detachment, macular perfusion indices, choriocapillaris subfoveal plexus, superficial vascular plexus, vessel density

Posted Date: April 8th, 2022

DOI: https://doi.org/10.21203/rs.3.rs-1534959/v1

Abstract

Background

Information about long term perfusional status of patients who have undergone successful surgery for giant retinal tear (GRT) macula-off rhegmatogenous retinal detachment (RRD) is limited.

Purpose

To examine long term perfusional, structural, and functional outcomes in normal control eyes and the eyes treated for different degrees of GRT-associated extensions of RRD.

Methods

One emmetropic normal eye (control), one healthy highly myopic eye (control myopic), and three eyes surgically treated for GRT (surgical), were included in the study for a long-term comparison of study outcomes. The surgical eyes were classified based on the degree of GRT-associated RRD extension as follows: One eye with GRT-associated RRD extension < 180°, one eye with GRT-associated RRD extension between 180°–270°; and one eye with GRT-associated RRD extension > 270°. Structural, functional, and perfusional outcomes were compared with those of control eyes.

Results

All three included eyes were phakic and the condition was monocular. The mean age of the patients was 48.67 ± 8.50 years (range, 39–55 years). All three eyes had GRT macula-off RRD. The mean preoperative time for GRT surgery was 1.2 weeks. The mean pre- and postoperative best corrected visual acuities (BCVA) were 1.87 logMAR and 0.46 logMAR, respectively. The mean postoperative follow-up period was 19.67 ± 5.69 months. Proliferative vitreoretinopathy (PVR) resulted in multiple surgeries in one eye (31.5%). Long-term postoperative optical coherence tomography (OCT) showed abnormal retinal thickness, ellipsoid zone (EZ) disruption, and external limiting membrane (ELM) line discontinuities in one eye. OCT angiography yielded abnormal perfusion indices in the surgically treated eyes.

Conclusions

Our data showed multiple structural alterations in spectral-domain OCT biomarkers. One eye that developed secondary epiretinal membrane (ERM) proliferation showed a significantly improved BCVA after proliferation, and the internal limiting membrane (ILM) were removed. Perfusional findings were correlated with final BCVA. Despite a fully reattached retina without ERM proliferation, GRT-associated RRD has a guarded functional prognosis.

Introduction

Rhegmatogenous retinal detachment (RRD) associated with giant retinal tears (GRTs) is an uncommon condition with a guarded prognosis as it may cause significant visual morbidity from retinal detachment [1]. GRTs-associated RRD is a tractional event, an acute condition, that is complicated by the vitreoretinal interface in which pathological contraction phenomena of the vitreous and the bed of a normal or predisposed retina cause a full-thickness circumferential retinal tear of > 90° associated with vitreous detachment [2, 3]. The high incidence of PVR from GRT is due to the release and fibrous metaplasia of high number of retinal pigment epithelial cells (RPE cell dispersion), inflammatory breakdown of the retina-blood barrier with upregulated release of multiple pro-inflammatory factors and cytokines resulting in a rapid occurrence of proliferative vitreoretinopathy (PVR) [1]. The annual incidence of GRT is not clearly established in the literature however it is estimated that between 0.05–0.09% per 100,000 people every year suffer from the condition [2–7]. GRT predominantly affects male gender, in up to 72% of total patients [2–7] - they represent 1.5% of the total RRDs, with an average age of 42 years at diagnosis [3, 6].

The formation of GRT is attributed to the combination of an area of retinal abnormality and dynamic vitreous traction [3]. The tear in the retina in GRT occurs acutely in different magnitudes. The severity is known to depend on the substrate and the condition of the eye [8]. The coalition of multiple horseshoe tears on the posterior border of the vitreous base due to several acute pathologic contraction of the vitreous may also be associated with the formation of GRTs. These pathologic conditions lead to the circumferential rupture of the retina greater than one peripheral quadrant (> 90° retina rupture).

Several risk factors may be the causation for these pathologic changes which include, local factors, systemic risk factors and some other unknown or secondary conditions [2, 3, 8–10]. A large epidemiologic study conducted in the United Kingdom (2010) found that approximately 55% GRTs are idiopathic. Other studies found the association of GRTs with several other ocular and systemic conditions: 25% are myopia-associated, 14% are associated with hereditary conditions with defects in type 2 collagen synthesis, such as Marfan's, Stickler–Wagner, and Ehrler Danlos syndromes, and 12.3% result from close-eye blunt trauma [2, 3, 8–10]. Other risk factors include high myopia, aphakia and pseudophakia [2, 3, 8–10]. Other more rare conditions that have been identified in GRT include aniridia, lens coloboma, microspherophakia, retinitis pigmentosa, and endogenous endophthalmitis [11].

In GRTs, the rate of anatomic success after the first surgery is between 80% and 90%, while the final reattachment rate is 94–100% [12, 13]. However, the condition is very difficult to manage due to the risks of several intra and postoperative complications. Additionally, several histopathological abnormalities may occur during surgical procedures, e.g., during scleral buckling surgery (e.g., placement of scleral buckle (SB), encircling bands, compression of the eyeball, and cryotherapy to the scleral vessels) may result in an interruption of the blood supply to the anterior segment of the eye [14–17].

The aim of this study was to evaluate the long term postoperative retinal and choroidal vasculature in eyes with GRT-associated macula-off RRD and those undergoing vitrectomy without scleral buckling using as seen in optical coherence tomography (OCT) angiography. It will help to improve the control-perfusion vitrectomy techniques without the probable deleterious effects of scleral buckling on retinal and choroidal perfusion. We compared the indices of macular microcirculation in normal emmetropic (Figs. 1a to 1k), normal healthy myopic (Figs. 1l, 1w), and operated eyes with GRT macula off RRD which resolved completely after vitrectomy surgery and minimized the confounding variables.

Patients And Methods

Study design

This study adhered to the tenets of the Declaration of Helsinki and was approved by the ethics and teaching committees of the enrolled institution. Written informed consent was obtained from all patients in accordance with institutional guidelines.

The three patients who fulfilled the following criteria were included in the surgical cohort, which included: age ≥ 18 years, having GRT-associated RRD, evidence of PVR grade B or less, retinal attachment at the last follow-up examination visit, absence of intraocular silicone oil in the last follow-up visit, at least six months of follow-up, and a well-documented long-term structural, functional, and perfusional findings of the macula during follow-up visits [18].

The following patients were excluded from the study: any prior complicated surgeries (e.g., vitreoretinal surgery or intravitreal injections), GRT-associated RRD (e.g., due to open eye injuries), GRT-associated RRD with a macular hole retinal detachment in myopic traction maculopathy (MTM). Other exclusion criteria included the presence of intraocular silicone oil during the final evaluation, PVR (posterior or anterior) with recurrent RRD, and presence of active glaucoma. Additionally, patients who could not maintain the follow up procedures and were operated in other than the included institution and with severe complications (e.g., endophthalmitis, recurrent disease, complicated severe PVR RRD, and refractory corneal opacities) were also excluded [18].

The assessments included: long-term postoperative structural spectral-domain (SD)-OCT findings including foveal contour profile, central subfoveal ellipsoid zone (EZ) status, central subfoveal external limiting membrane (ELM) line appearance, en-face imaging or cross-sectional SD-OCT B-scan analysis for the presence of dissociated optic nerve fiber layer (DONFL) defects, and the presence of epiretinal membrane (ERM) proliferation over the macula. Postoperative macular perfusion evaluation included vessel density (VD) at the superficial vascular plexus (SVP), deep vascular plexus (DVP), foveal avascular zone (FAZ), and choriocapillaris subfoveal plexus (CSP). The BCVA in Snellen unit was converted to logMAR units using standard formulas.

The clinical charts of the included patients, with a diagnosis of GRT-associated with RRD and treated between May 2017 and January 2021 were included and interpreted. Only eyes with a fully attached retina and functional vision on the patients’ last postoperative evaluation, regardless of the number of surgical procedures needed, were selectively included. Thus, three selected eyes from three patients were included and classified according to the circumferential size of the GRT. One eye had RRD associated with circumferential retinal tears of < 180°, one eye had RRD associated with circumferential retinal tears between 180° and 270°, and one eye had RRD associated with circumferential GRTs of > 270°. The postoperative eyes were analyzed statistically to demonstrate the postoperative functional, structural, and perfusional macula-off retinal detachment outcomes. Only eyes in which the retina was successfully reattached without the presence of intraocular silicon for a minimum of six months of follow-up after the last vitreoretinal surgical procedure were included in the general dataset.

Examinations

A detailed eye examination was carried out in all included participants, which included preoperative evaluations such as visual acuities, slit-lamp examination, fundoscopy, and indirect ophthalmoscopy. The assessment protocols used in these cases have been reported previously [18]. In brief, cross-sectional images of the macular region were acquired along the horizontal plane through the foveal center using Spectralis OCT (Heidelberg Engineering, Heidelberg, Germany) or, in some cases, SD-OCT (RTVue-XR platform SD-OCT, Optovue Inc., Fremont, CA, USA), and the axial lengths were measured using partial coherence laser interferometry (Zeiss IOL Master 700; Carl Zeiss Meditec AG, Oberkochen, Germany). GRT-associated with RRD was diagnosed through indirect ophthalmoscopy and B-scan ultrasonography (A and B Ultrasound Unit, Quantel Medical, Du Bois Loli, Auvergne, France). The postoperative microstructural evaluation was performed using SD-OCT Spectralis OCT and RTVue-XR platform SD-OCT. The following postoperative structural and perfusional assessments of the eyes were statistically analyzed in three groups: long-term postoperative structural spectral-domain (SD)-OCT findings including central subfoveal thickness (CSFT), foveal contour profile, central subfoveal ellipsoid zone (EZ) status, central subfoveal external limiting membrane (ELM) line appearance, en-face imaging or cross-sectional SD-OCT B-scan analysis for the presence of dissociated optic nerve fiber layer (DONFL) defects, and the presence of ERM proliferation over the macula.

Postoperative perfusion and quantitative VD and choroidal flow evaluations were completed using an OCT angiography device (RTVue XR OCT Avanti with AngioVue Software; OptoVue Inc., Fremont, CA, USA). More details about the equipment can be found elsewhere [19]. Default retinal imaging settings and built-in projection artifact removal tools were used to perform image adjustment and segmentation. Segmentation of the SVP, DVP, outer retinal layer, and CSP slabs was performed using AngioVue software. The imaging data were interpreted by an independent analyst. Scan quality was evaluated using the standard signal strength index (SSI) provided by the software, and only scans with an SSI > 46 were included.

The procedure for image analysis was done following a published protocol [19]. In brief, the FAZ area in the SVP slab was quantitatively evaluated by analysing images in the AngioVue system. A built-in tool in the AngioVue system measured the VD [20, 21]. All multimodal evaluations and images were analyzed by three experienced retina specialists (co-authors) from the participating institution.

Surgical technique

Surgical technique performed in these patients was described in detail previously [18]. In brief, standard 25-gauge 3-port pars plana vitrectomy (Alcon Constellation Vision System, Alcon Labs, Fort Worth, TX, USA) was performed using a contact wide-angle viewing precorneal lens system (ROLS reinverted system Volk Medilex, Miami, FL, USA) or the Wide-Angle Viewing System (WAVS) with the resight non-contact lens (Carl Zeiss Meditec AG, Jena Germany). In addition to central vitrectomy, we use diluted triamcinolone acetonide adjuvant (Kenalog 40 mg/mL; Bristol-Myers Squibb, New York, NY, USA) to better visualize the vitreous face, vitreous base, and its posterior border, and perform a removal of the cortical face from the surface of the retina using a silicone-tipped cannula with active suction prior to perfluorocarbon liquid (PFCL) infusion and reattachment of the retina. A subretinal fluid (SRF) endodrainage was performed as described previously [18]. In brief, endodrainage was done slowly by implementing a first-step air-to-fluid exchange over the edge of the GRT to avoid posterior retinal slippage before proceeding to a second air-fluid exchange and continuing with SRF drainage. Once the retina was completely reattached, continuous argon laser endophotocoagulation was performed. Finally, as the last surgical step, a non-expandable bubble containing 15% perfluoropropane (C_3F_8) gas mixture was used as a long-acting tamponade at the end of the procedure in the three cases, as previously described [18].

Statistical analysis

Data were entered and processed using Microsoft Excel and analyzed using GraphPad Prism version 8.2.1 and SPSS for Windows version 28. Data were assessed for normal distribution and appropriate Statistical tests selected. Spearman’s correlation test was used to compare perfusion indices with the final visual outcome. Wilcoxon matched signed-rank test was used to compare the preoperative and postoperative BCVA values in the surgical group (logMAR). For functional evaluations among the stages and surgical variants, only the final postoperative BCVA was included in the statistical analysis. Statistical significance was set at $p < 0.05$.

Eyes were divided according to tear magnitude: with a GRT < 180°, of 180–270°, and > 270°. The Kaplan–Meier method was used to evaluate the general survival for final postoperative BCVA logMAR units between the divided eye groups.

Results

The clinical charts of 3 consecutively selected patients who were surgically managed between January 2015 and May 2021 were analyzed. Only eyes with a fully attached retina and functional vision on the patients’ last postoperative evaluation, regardless of the number of surgical procedures needed, were selectively included. Thus, 3 eyes from 3 patients were included and classified according to the circumferential size of the GRT. The postoperative eyes were analyzed statistically to demonstrate the functional, structural, and perfusional macula-off retinal detachment outcomes.

Only eyes in which the retina was successfully reattached without the presence of intraocular silicon for a minimum of six months of follow-up after the last vitreoretinal surgical procedure were included in the general dataset.

Outcome measures

Macular quantitative perfusion indices (superficial and deep vessel density at different subdivided sections of the macula), structural outcomes and functional improvements were compared in terms of logarithm of the minimum angle of resolution (logMAR) units. Anatomical success was defined by a disappearance of RRD without new retinal tears, clinically and tomographic resolution of the macular SRF, or reattachment of the retina before the final visit regardless of the number of surgical procedures. The SD-OCT findings at the last follow-up evaluation were used to perform statistical microstructural comparisons; assessment of the long-term OCT angiography perfusion indices was performed in the last visit. Data were collected by two other macula and retina specialists masked to other information - only a third observer evaluated the SD-OCT readings in case of disagreements.

General Outcome

No evidence of PVR or other postoperative complications was found in the eye with GRT-associated RRD extension < 180°. The postoperative BCVA (0.48 logMAR) was significantly better than the preoperative BCVA (2.00 logMAR) (Table 1). In the eye with GRT-associated RRD extension = 180°–270, the pre- and post-operative BCVA were 1.60 logMAR and 0.30 logMAR, respectively. In the eye with GRT-associated RRD extension > 270°, the pre- and post-operative BCVA was 2.00 logMAR, and 0.60 logMAR, respectively (Table 1).

Table 1
Patients’ demographic data and pre-operative clinical characteristics

Study groups	Age	Preoperative BCVA (logMAR units)	Axial length (mm)	Post-operative follow-up months
Control emmetropic eye (n = 1)	54	0.00	20.32	-
Control myopic eye (n = 1)	62	0.00	29.12	-
Surgical group (n = 3)				
GRT < 180º	55	2.00	22.54	18
GRT 180–270º	52	1.60	26.38	26
GRT > 270º	39	2.00	30.10	15

BCVA, best-corrected visual acuity

Structural analysis among eyes

To describe the structural postoperative spectral domain-optical coherence tomography (SD-OCT) findings (Table 2), we used the terminology proposed by the International Nomenclature for Optical Coherence Tomography Panel report, [22] which correlated with the functional findings. The statistical program yielded the following SD-OCT findings: foveal contour (33.3%), EZ disruption in 33.3%, DONFL abnormalities in 33.3%, and ELM line alterations in 33.3% of the eyes. The differences between these categorical variables were not statistically significant ($p > 0.05\%$) (Table 2).

Table 2
Comparison between tear magnitude groups to measure the associations from the other study variables

	Sample	Tear < 180°	Tear 180–270°	Tear > 270°
	N = 3	N = 1	N = 1	N = 1
Foveal contour				
Normal	2 (66.6%)	1	1	
Abnormal	1 (33.3%)			1
Ellipsoid zone				
Normal	2 (66.6%)	1	1	
Disrupted	1 (33.3%)			1
DONFL defects				
Absent	2 (66.6%)	1	1	
Present	1 (33.3%)			1
ELM line				
Normal	2 (66.6%)	1	1	
Disrupted	1 (33.3%)			1

DONFL, dissociated optic nerve fiber layer; ELM, external limiting membrane; ERM, epiretinal membrane

Perfusional analysis among eyes

The superficial FAZ area in the control emmetropic eye was significantly smaller than that in the other eyes. The superficial foveal VD in the emmetropic eye differed only from that of the eye with GRT-associated RRD extension = 180°–270° and that in eyes with GRT-associated RRD extension > 270°. Deep foveal VD differed only between the emmetropic eye and the eye with GRT-associated RRD extension of > 270°. The flow area in the CSP was significantly larger in the emmetropic group.

Decreased superficial foveal VD correlated with poor visual outcome in eyes with GRT-associated RRD extension > 270°. Similarly, a smaller flow area in the CSP was associated with poorer visual outcomes in eyes with GRT-associated RRD extension > 270° (Table 3).

Table 3
Comparative functional, structural and quantitative evaluation of macular perfusion indices across study eyes

Study groups	Superficial FAZ area (mm^2)	Superficial foveal VD (%)	Deep foveal VD (%)	Superficial parafoveal VD (%)	Deep parafoveal VD (%)	Superficial whole macula VD (%)	Deep whole macula VD (%)	Flow area (mm^2) at Choriocapillaris subfoveal plexus	CSFT (μm)	Post-Op BCVA
Control emmetropic	0.31	32.17	32.29	57.72	58.27	57.83	57.40	2.54	242.40	0.00
Control high myopia	0.53	31.77	33.21	56.34	55.88	47.45	49.45	2.45	254.3	0.00
Surgically treated (n = 3)										
GRT < 180º	0.89	27.93	30.22	47.69	49.23	49.13	49.35	1.95	206.9	0.48
GRT 180–240º	1.42	20.07	24.40	35.21	37.22	39.22	40.26	1.24	190.0	0.30
GRT < 270º	1.83	21.54	22.68	25.72	28.91	30.11	32.39	1.36	204.8	0.60

*Indicates where data differed significantly ($p < 0.05$) from the control emmetropic eye. The BCVA in the control emmetropic and control high myopia eyes was used for comparison with postoperative BCVA in the surgical group. Abbreviations- FAZ; foveal avascular zone, VD; vessel density, CSFT; central subfoveal thickness.

A Kaplan –Meier survival probability plot was included for tear magnitude. Each plot represents the survival probability of different groups over time (Fig, 2).

Surgical Cases

Surgical case 1

A 55-year-old phakic, symptomatic woman presented with complaints of metamorphopsia and sudden visual loss in her right eye. The vision loss occurred over a period of seven days. Preoperative right eye visual acuity was 20/2000 (logMAR 02.00); refractive error of -2.00 + 1.25x10 and axial length of 22.54 mm, ocular tension by applanation tonometry of 10 mmHg. The evaluation of the fundus showed a total detachment of retina due to a giant tear of the meridian from VIII meridian to I meridian, with clear media, vitreous liquefaction and with a large amount of pigment granules. The tear bent on itself allowing to observe a large amount of subretinal fluid beneath the macula (Fig. 2a). Multiple areas of thinning were detected in the retina with some liquid sockets and areas of vitreoretinal traction. The patient underwent uneventful gas-vitrectomy, no scleral cerclage was installed, and 15% C3F8 gas injection, the evolution was satisfactory, keeping the retina attached and recovering visual acuity in a satisfactory way. At eighteen months of follow-up, the final BCVA was 20/60 (logMAR 0.48). Several SD-OCT biomarkers were noted, such as an irregular foveal contour and internal and external neuroretina lines without total restoration of the central subfoveal ellipsoid, such as at the EZ and the ELM line (Fig. 2b). The long-term postoperative perfusion evaluation was abnormal with lower-than-normal perfusion indices on the SVP (Fig. 2c) and DVP slabs (Fig. 2d). The perfusional indices were quantified and considered lower than normal (Fig. 2e, f, g, h). The choriocapillaris flow area was considered in range with 2.113 mm^2 (Fig. 2i) with an enlarged and irregular FAZ area of 4.036 mm^2 (Fig. 2j)

Surgical case 2

A 52-year-old phakic, symptomatic woman presented with complaints of aggravating metamorphopsia, and entopic phenomena; these were accompanied by a progressive and rapid drop in central vision, and high myopia. The right eye with an axial length of 26.38 mm and a GRT macula off associated RRD of 200-degree extension over the temporal and superior quadrants (Fig. 3a) underwent an uneventful gas-vitrectomy surgery (Fig. 3A). The preoperative BCVA was measured at 20/800 (logMAR 1.60). We performed a three-port 25-G pars plana vitrectomy and perfluorocarbon liquid assisted technique to flatten the retina and do the endodrainage of subretinal fluid. Fluid-air gas exchange was performed with 15% C_3F_8 tamponade. After a 26-month longitudinal follow-up (Fig. 3b), the operated eye showed a postoperative BCVA of 20/40 (logMAR 0.30). The long-term high-definition 12 mm structural b scan evaluation exhibit an irregular foveal profile with well recognized outer retina biomarkers (Fig. 2c and d). The postoperative perfusion indices at the SVP (Fig. 3e) and DVP slabs (Fig. 3f) were considered below mean with no evidence of epiretinal membrane (ERM) proliferation. The quantified perfusion indices at the different subregions of the macula along with the retinal thickness were lower than normal (Fig. 3g). Color overlays on the OCTA angiography images indicating superficial (Fig. 3h) and deep (Fig. 3i) quantified VD values at the different subregions of the macula seen in the key to the right and above the images were considered lower than normal.

Surgical case 3

A 39-year-old man with two days of sudden decrease vision with metamorphopsia, high myopia, and severe PS. The patient was diagnosed of having a familiar condition consistent with Stickler´s syndrome by the genetic unit. The diagnosis of a GRT-associated RRD of more than 270-degree extension was made (Fig. 4a and b). The preoperative BCVA was 20/2000 or counting fingers at 2 feet (logMAR 2.00), with PS and an axial length of 30.10 mm. This right phakic eye underwent a 25-G three-port pars plana gas-vitrectomy. Because of recurrent and a complicated proliferative vitreoretinopathy (PVR) RRD, this eye underwent a second surgical procedure consistent of vitrectomy revision and macular surgery consisting of BBG dye-assisted ERM/ILM peeling en-bloc removal technique and silicon oil injection. Lighter than water silicon oil was uneventfully removed four months later. After a 15-month follow-up, the final postoperative BCVA was 20/80 (logMAR 0.60) and showed a SD-OCT pattern consistent with an abnormal macular profile and presence of abnormal biomarkers such as inner and outer retina SD-OCT layers, abnormal subfoveal EZ and ELM line discontinuities with a well-preserved RPE layer (Figs. 4c and d), the en-face aspect depicted multiple deep defects at the level of the RPE with a very abnormal perfusion evaluation on the SVP slab (Fig. 4e) with better perfusion evaluation on the DVP slab (Fig. 4f). The superficial (Fig. 4g) and deep (Fig. 4h) perfusional indices and corresponding retinal thickness values at different subregions of the retina were lower than normal. Color overlays on the OCTA angiography images indicate superficial (Fig. 4I) and deep (Fig. 4j) lower than normal quantified VD values at the different subregions of the macula seen in the key to the right and VD percentage of the perfusion indices above the images were considered lower than normal. The choriocapillaris flow was very deficient with 1.366 mm^2 of flow from a selected area of 3.142 mm^2 (Fig. 4k). The FAZ area looked irregular and enlarged with 9.657 mm^2 in area (Fig. 4l). The last long-term structural crossline SD-OCT b scan evaluation showed irregular foveal profile, irregular diffuse retinal thinning over the temporal and inferior side of the macula in both horizontal and vertical b scans respectively, evidence of dissociated optic nerve fiber defects and irregularities of the outer retina layers biomarkers (Fig. 4m).

Discussion

Benefits of adding an encircling scleral buckle (SB) to vitrectomy for GRT-associated RRD are still largely unknown [23, 24]. Some authors claim that due to abnormal vitreous base and decreasing support of tractional forces in that region could cause the break which leads to GRTs [25–27]. In GRTs-associated RRD, SB procedure is thought to be controversial for its placement before reattachment of the retina. Due to several potential consequences, such as chances of the removal of anterior vitreous or posterior slippage of the retina, and additionally potential damage to the retinal and choroidal microcirculation, this case report included only the eyes that were operated previously without scleral buckling procedures. Some authors believe the buckling to be an integral part of the surgical step as it helps to relieve the tractional forces at the edges of the tears and thus providing supporting to the vitreous base [27]. Our analysis from long term postoperative perfusion findings suggests a time-related change in perfusion density. The data showed a reduced perfusion (both retinal and choroidal) after the control-perfusion vitrectomy technique. There was also a uniform reduction in the choroidal vessel network, which was evident in the topographical sub-analysis of the flow area. Several histopathological harmful consequences are reported previously due to surgical maneuvers, regarding placing scleral buckles, which we could avoid [23, 24]. Cases with a complementary SB were purposefully excluded due to the chances of their influence on the perfusion state of the microvasculature system of the retina and choroid.

Retinal surgeons have some consensus which led to the idea of using SB in GRTs < 180°, especially when there is not PVD and retinal folding. However, other retinal surgeons think that it may not be a proper technique because GRT > 180° increase the chances of vitreous traction. Therefore, SB may not have any benefits but increases the chances of complications. The long term perfusion status was evaluated as done by previous researchers [28]. A sustained vessel density due to enhanced perfusion can improve vision and prevent its deterioration [29]. Also, myopic eyes with decreased choroidal perfusion may attribute to the mechanical stretch forces that arise due to elongation of the eyeball [30]. However, this fact could not be proven in our case series.

Based on our observations, and also from the literature, it is evident that assessment of microcirculation has a key clinical benefit [29], especially because in several diseases such as retinal vascular diseases, including diabetic retinopathy, macular telangiectasia, and radiation retinopathy, small vessel changes with lower vessel density have been well documented [23, 31, 32].

OCT angiography quantitative perfusion indices can reproducibly facilitate the detection of postoperative structural outcomes. We observed that visual acuities were correlated to the flow area of the CSP slabs. However, the small sample size limited us from making other significant observations and comparisons. However, we compared normal-range vessel changes in three groups of eyes: normal emmetropic, healthy, highly myopic, and eyes with different degrees of GRT-associated extensions of RRD. We observed differences in macular perfusion indices between the control eyes and GRT-related RRD. Significant differences were found when the microcirculation of the macula was analysed using quantitative VD perfusion indices. These perfusion deficiencies suggest a possible causal relationship between the perfusion mechanisms and lack of better visual recovery in this condition [18]. Similar effects have been published by Christou, [33] which suggest postoperative OCT angiography findings to be a hypothetical explanation of suboptimal vision recovery without current evidence to establish OCT angiography biomarkers as predictive factors.

Our case studies provide support for the role of microcirculation as a fundamental player in postoperative visual recovery. Several studies have directly examined the correlation between choroidal perfusion and VD. Care should be taken to avoid reduction of the choroidal perfusion in eyes with GRTs associated with RRD due to surgical changes (e.g., by compression of the choroid secondary to buckling surgery) [33]. FAZ distortion with enlargement of the juxtafoveal capillary net contributes to decreased VD perifoveal perfusion indices in the different stages of MTM [19]; this fact should be proven in successfully operated GRT-associated RRD eyes.

We observed a positive correlation between BCVA and macular perfusion indices across different degrees of GRT-associated extensions of RRD, which suggest that VD flow abnormalities (lower value of choroidal thickness), may correspond to lack of visual recoveries. It is important to note that the current control-perfusion vitrectomy techniques performed in this study are crucial to reversing the state of the eye. Similarly, it is important to complete the reattachment procedures for the retina by avoiding complications, that are imminent. In our cases, early performance of the procedure prevented future damage to the eye. However, patients with a tear magnitude of 180º-270º had the best probability of survival, while patients with a tear magnitude > 270º had the worst survival rate. Thus, these patients must be treated quickly to avoid irreversible visual damage.

We did not apply endolaser even for GRTs with extents < 180° because there is no evidence in the literature to add 360° endolaser when there is no lattice degeneration [26]. However, we performed extensive assisted-vitreous base shaving. Fluid-air exchange is arguably the most critical step in the surgical repair of GRT-associated RRDs, and an improper technique can result in retinal slippage or retinal fold formation. Meticulous, slow aqueous removal with an extrusion cannula at the air-PFCL interface and at the edge of the tear is essential. We did not observe any occurrence of macular retinal folds due to posterior slippage in eyes with GRTs extending < 180° or in GRTs extending > 180°. Also, we could not study the benefits of SB in our surgeries as we did not include those cases although some surgeons insist on using this technique while others do not [25]. We also did not use short-acting gas (sulfur hexafluoride) in our patients because they are known to cause re-detachment to a higher rate [34]. However, we used C_3F_8 in all cases regardless the extent of GRT. Silicon lighter than water was used as a tamponade only in an eye with PVR, which was eventually removed while preserving the attached retina. Several factors lead to the decision to the choice of a tamponade agent. For example, Kunikata *et al.* [35] used silicone oil as a tamponade in 34 of 41 eyes (83%) with GRT-associated RRD.

The risk factors that cause the recurrence of RRD include anterior PVR and persistent or new epiretinal traction at the corners of the tear [1, 2]. We observed RRD recurrence in one patient due to posterior PVR with evidence of postoperative ERM proliferation over the detached macula. We believe that it contributed to the creation or activation of new tears through diffuse posterior epiretinal traction. The eye with recurrent RRD underwent vitrectomy revision, epiretinal and macular membrane stripping, and ERM/ILM en-bloc removal during follow-up.

The rate of reattachment following one procedure is 80–90%, while the final reattachment rate is 94–100% [12, 36]. However, if PVR is present, the visual prognosis is poor despite reattachment and anatomic success, as was demonstrated here and in a previous study [2]. In contrast, other researchers have reported that the most common postoperative complications occurred in 16 eyes (39%), including macular ERM proliferation and cystoid macular edema [35]. reported that Some authors believe that [36] good anatomical and functional results can be obtained only with vitrectomy techniques in non-complex cases. In our study, we observed a 66.7% rate of reattachment after one surgical procedure, which is consistent with the 65% rate at two years (95% confidence interval: 47%, 78%) reported by Li et al. [36].

A prospective study reported that even eyes that underwent timely surgery hardly achieved a recovery of vision of 20/40 or better, highlighting the difficult management of the condition, [37]. We believe that the absence of SB does not seem to influence the final functional results, as seen in our data. In fact, the factors that lead to poor visual outcomes include old age (over 70 years), low IOP (less than 10 mmHg), retinal detachment with more than four rhegmatogenous lesions, and retinal detachment of more than three quadrants [37]. However, it is now clear that the final visual outcome is correlated to the perfusion indices. Therefore, we hypothesize that both the extensive pathological rupture of the retina as well as the vitrectomy techniques can potentially damage the microcirculation of the retina and choroid, resulting in low rates of perfusion and unsatisfactory postoperative vision. We did not find any association between number of breaks, lens extraction, additional cryotherapy and the type of surgery (primary vitrectomy vs. combined SB and vitrectomy techniques) to affect the anatomic success, which is also reported by Ting et al. [38]. In our study, the postoperative BCVA in logMAR units was significantly associated with the CSFT in microns, the normal foveal contour, and the abnormal perfusion indices according to our statistical analysis. We observed that the thinner the CSFT and lower the perfusion indices, the lower the postoperative BCVA. The preoperative logMAR was higher in tear > 270º and the final postoperative logMAR was lower in the same eye. The results of this study reaffirm the hypothetical concept of the author that the greater the extent of the giant tear, the less need to place a scleral buckle; the previous clinical fact supported by our results where the worst perfusional indices were observed precisely in giant tears greater than 180 treated with complementary scleral cerclage and this outcome positively correlates with the worst final BCVA.

This study has several limitations, mainly its retrospective nature and low sample size. However, there were several inherent strengths, such as its long-term follow-up evaluation. Additionally, the data reported here are from a single surgeon, which eliminated the surgeon-bias factor. Also, the paucity in the data on a relatively rare condition of GRT-associated RRD allowed us to correlate functional and structural outcomes with perfusional outcomes, which has been explored very little previously.

Conclusion

To conclude, GRT-associated RRD remains a potentially blinding condition with limited final functional outcomes despite advances in management techniques of this condition. The advancement in technology has improved our understanding of the anatomical structures and the ways to treat the disease however, the assessment of perfusion status is still a new concept. Although surgical timing is important in reducing long-term complications, minimizing the complication rate, and improving the reattachment rate. Patients enrolled for a long duration to evaluate the long-term perfusion and functional outcomes from these patients suggest a role of these indices in better patient management. Additionally, as GRT-associated RRD is a rare condition, the data presented here have significant clinical implication. The most important outcomes of this study concerning the management of GRT-associated RRD include the benefits of thorough control-perfusion vitrectomy with the postoperative findings in macular perfusion indices in eyes, which allowed us to conclude the importance of begin to evaluate pre- and postoperative macular perfusion indices in these patients in order to perform surgical techniques with transoperative control of perfusion and preferably without the assistance of complementary scleral cerclages that accordingly to published clinical evidence are unnecessary and potentially harmful to retinomacular perfusion.

Abbreviations

BBG; Brilliant Blue G; BCVA, best-corrected visual acuity; CSP, choriocapillaris subfoveal plexus; CSFT, central subfoveal thickness; DVP, deep vascular plexus; DONFL, dissociated optic nerve fiber layer; VD, vessel density; ELM, external limiting membrane; ERM, epiretinal membrane; GRT, giant retinal tear; ILM, internal limiting membrane; OCT, optical coherence tomography; PFCL, perfluorocarbon liquid; PVD, posterior vitreous detachment; PVR, proliferative vitreoretinopathy; RD, retinal detachment; RPE, retinal pigment epithelium; RRD, rhegmatogenous retinal detachment; SB, scleral buckle SD, spectral domain; SS, swept source; SRF, subretinal fluid; SB, scleral buckle; SVP, superficial vascular plexus; WAVS, wide-angle viewing systems. WWOP, white without pressure

Declarations

Acknowledgements

We express our appreciation to the technical staff of the Retina Specialists Unit at Oftalmologia Integral ABC in Mexico City. Mexico, which is affiliated with the postgraduate division of studies at the National Autonomous University of Mexico. Images a to d and images i to l in Fig. 1; images j to l in Fig. 2; images a–b and images d–l in Fig. 3; images a, b, d, e and h to l in Fig.4; and images a, d, and g in Fig. 5 were generously contributed by Alejandra Nieto-Jordan, Jennifer H. Kim-Lee, Felipe Correa-Esparza, and the retina service of the Institute of Ophthalmology. We especially thank Jorge Morales-Navarro for his valuable statistical contributions. Valuable academic contributions were made by Alejandra Nieto-Jordan, Felipe Esparza-Correa, Boris Moreno-Andrade for which we give our sincere recognition and gratitude. All patients underwent surgery in both campuses of the Centro Medico ABC and the Institute of Ophthalmology operating room facilities.

Ethics approval and consent to participate

This retrospective study adhered to the tenets of the Declaration of Helsinki, received full ethical approval from the research ethics committee, and was approved by the institutional review committee and teaching department of the institution (no reference numbers were provided for retrospective studies by this institution). Written informed consent was obtained from all patients in accordance with institutional guidelines.

Consent for Publication

The authors affirm that the participants provided informed consent for the publication of all images in Figures 1 to 4 from selected patients, as well as the images in the online resources, if any.

Availability of data and materials

Datasets supporting the conclusions of this study are included in the article. *Dr. Miguel A. Quiroz-Reyes states that he has no financial disclosures relevant to this article. He may be contacted through* drquiroz@prodigy.net.mx *and* drquirozreyes7@gmail.com.

Photos and composite figures supporting the findings of this report may be released by written application to the Photographic Laboratory and Clinical Archives Department of the Retina Specialists Unit at Oftalmologia Integral ABC. Medico-surgical assistance institution (non-profit organization). Av. Paseo de las Palmas 735 suite 303. Lomas de Chapultepec. Mexico City 11000, Mexico, and the corresponding author upon request.

Competing interests

The authors declare that they have no competing interests.

Funding

No funding or grant support was received for this study.

Authors' contributions

Dr. Quiroz-Reyes MA had full access to all of the data in the study and takes responsibility for the integrity of the data and the accuracy of the data analysis. Concept and design: Quiroz-Reyes MA; Quiroz-Gonzalez EA. Drafting of the manuscript: Quiroz-Reyes MD. Acquisition analysis, dataset interpretation. Ahmad R Alsaber: Acquisition analysis, statistical analysis. Final revision, conclusions: Quiroz-Reyes MA, Lima-Gomez V. Figures artwork, tables, photographic material compilation: Quiroz Gonzalez EA.   Assistant surgeon: Quiroz-Gonzalez MA. Photographic material compilation: Montano, M. Critical revision of the manuscript for important intellectual content: Quiroz-Reyes MA, Lima-Gomez V, All the authors have approved the manuscript for submission.

Co-Authors Affiliation

All co-authors but Ahmad R Alsaber are affiliated to the Faculty of Medicine in the Postgraduate Studies Division at NATIONAL AUTONOMOUS UNIVERSITY OF MEXICO. Mexico City, Mexico.

References

1. Ang, G.S., J. Townend, and N. Lois, *Interventions for prevention of giant retinal tear in the fellow eye.* Cochrane database of systematic reviews, 2009(2).

2. Ang, G.S., J. Townend, and N. Lois, *Epidemiology of giant retinal tears in the United Kingdom: the British giant retinal tear epidemiology eye study (BGEES)*. Investigative ophthalmology & visual science, 2010. **51**(9): p. 4781-4787.

3. Shunmugam, M., G.S. Ang, and N. Lois, *Giant retinal tears.* Survey of ophthalmology, 2014. **59**(2): p. 192-216.

4. Freeman, H., *Fellow eyes of giant retinal breaks.* Transactions of the American Ophthalmological Society, 1978. **76**: p. 343.

5. Wood, M.L. and C. Gilbert, *Retinal detachment in East Africa.* Ophthalmology, 2002. **109**(12): p. 2279-2283.

6. Chou, S., et al., *Characteristics of primary rhegmatogenous retinal detachment in Taiwan.* Eye, 2007. **21**(8): p. 1056-1061.

7. Malbran, E., et al., *Retinal break type and proliferative vitreoretinopathy in nontraumatic retinal detachment.* Graefe's archive for clinical and experimental ophthalmology, 1990. **228**(5): p. 423-425.

8. Ghosh, Y., et al., *Surgical treatment and outcome of patients with giant retinal tears.* Eye, 2004. **18**(10): p. 996-1000.

9. Nagpal, M., *Giant retinal tears: Size does matter.* Retina Today, 2013: p. 26-28.

10. Asaria, R.H.Y., et al., *Adjuvant 5-fluorouracil and heparin prevents proliferative vitreoretinopathy: results from a randomized, double-blind, controlled clinical trial.* Ophthalmology, 2001. **108**(7): p. 1179-1183.

11. Cahill, M.T., P.J. Barry, and P.F. Kenna, *Giant retinal tear in Usher syndrome type II: coincidence or association?* Retina (Philadelphia, Pa.), 1998. **18**(2): p. 177-178.

12. Sharma, A., V. Grigoropoulos, and T. Williamson, *Management of primary rhegmatogenous retinal detachment with inferior breaks.* British journal of ophthalmology, 2004. **88**(11): p. 1372-1375.

13. Pitcher, J., et al., *Giant retinal tear detachments: surgical strategies and outcomes.* Investigative Ophthalmology & Visual Science, 2013. **54**(15): p. 2864-2864.

14. D'Aloisio, R., et al., *Changes in iris perfusion following scleral buckle surgery for rhegmatogenous retinal detachment: an anterior segment optical coherence tomography angiography (AS-OCTA) study.* Journal of Clinical Medicine, 2020. **9**(4): p. 1231.

15. Hassan, T.S., et al., *The effect of duration of macular detachment on results after the scleral buckle repair of primary, macula-off retinal detachments.* Ophthalmology, 2002. **109**(1): p. 146-152.

16. Kwartz, J., et al., *Anterior segment ischaemia following segmental scleral buckling.* The British Journal of Ophthalmology, 1994. **78**(5): p. 409.

17. Doi, N., A. Uemura, and K. Nakao, *Complications associated with vortex vein damage in scleral buckling surgery for rhegmatogenous retinal detachment.* Japanese journal of ophthalmology, 1999. **43**(3): p. 232-238.

18. Quiroz-Reyes MA, Quiroz-Gonzalez EA, Quiroz-Gonzalez MA, Alsaber AR, Montano M,

et al. (2022) *Critical Analysis of Postoperative Outcomes in Rhegmatogenous Retinal Detachment Associated with Giant Tears: A Consecutive Case Series Study*. Int J Ophthalmol Clin Res 9:134. doi.org/10.23937/2378-346X/1410134

19. Quiroz-Reyes, M., et al., *Structural and Perfusional Findings in Surgically Resolved Myopic Foveoretinal Detachment Eyes and those in Early Stages of Myopic Traction Maculopathy.* J Clin Exp Ophthalmol, 2021. **12**: p. 893.

20. Klufas, M.A., et al., *Optical coherence tomography angiography reveals choriocapillaris flow reduction in placoid chorioretinitis.* Ophthalmology Retina, 2017. **1**(1): p. 77-91.

21. Kuehlewein, L., et al., *Optical coherence tomography angiography of type 1 neovascularization in age-related macular degeneration.* American journal of ophthalmology, 2015. **160**(4): p. 739-748. e2.

22. Staurenghi, G., et al., *International Nomenclature for Optical Coherence Tomography (IN• OCT) Panel. Proposed lexicon for anatomic landmarks in normal posterior segment spectral-domain optical coherence tomography: the IN• OCT consensus.* Ophthalmology, 2014. **121**(8): p. 1572-1578.

23. Ogasawara, H., et al., *Retinal blood flow alterations associated with scleral buckling and encircling procedures.* The British Journal of Ophthalmology, 1992. **76**(5): p. 275.

24. Diddie, K.R. and J.T. Ernest, *Uveal blood flow after 360 constriction in the rabbit.* Archives of Ophthalmology, 1980. **98**(4): p. 729-730.

25. Goezinne, F., et al., *Low redetachment rate due to encircling scleral buckle in giant retinal tears treated with vitrectomy and silicone oil.* Retina, 2008. **28**(3): p. 485-492.

26. Verstraeten, T., et al., *Lens-sparing vitrectomy with perfluorocarbon liquid for the primary treatment of giant retinal tears.* Ophthalmology, 1995. **102**(1): p. 17-20.

27. Lakhanpal, R.R. and S.M. Hariprasad, *Strategic planning ensures surgical success in cases of proliferative vitreoretinopathy.* Ophthalmic Surgery, Lasers and Imaging Retina, 2015. **46**(2): p. 155-157.

28. Wang, S.-W., et al., *Biomarkers in the pathogenesis of epiretinal membrane and myopic traction maculopathy: Effects of internal limiting membrane incompliance and posterior staphyloma.* Photodiagnosis and Photodynamic Therapy, 2021. **33**: p. 102208.

29. Kumagai, K., et al., *Factors correlated with postoperative visual acuity after vitrectomy and internal limiting membrane peeling for myopic foveoschisis.* Retina, 2010. **30**(6): p. 874-880.

30. Al-Sheikh, M., et al., *Quantitative OCT angiography of the retinal microvasculature and the choriocapillaris in myopic eyes.* Investigative ophthalmology & visual science, 2017. **58**(4): p. 2063-2069.

31. Sakata, K., et al., *Relationship between macular microcirculation and progression of diabetic macular edema.* Ophthalmology, 2006. **113**(8): p. 1385-1391.

32. Chin, E.K., et al., *Staging of macular telangiectasia: power-Doppler optical coherence tomography and macular pigment optical density.* Investigative ophthalmology & visual science, 2013. **54**(7): p. 4459-4470.

33. Christou, E.E., et al., *Association of OCT-A characteristics with postoperative visual acuity after rhegmatogenous retinal detachment surgery: a review of the literature.* International Ophthalmology, 2021. **41**(6): p. 2283-2292.

34. Gonzalez, M.A., et al., *Surgery for retinal detachment in patients with giant retinal tear: etiologies, management strategies, and outcomes.* Ophthalmic Surgery, Lasers and Imaging Retina, 2013. **44**(3): p. 232-237.

35. Kunikata, H., et al., *Successful surgical outcomes after 23-, 25-and 27-gauge vitrectomy without scleral encircling for giant retinal tear.* Japanese Journal of Ophthalmology, 2020. **64**(5): p. 506-515.

36. Li, K.X., et al., *Contemporary Management of Complex and Non-Complex Rhegmatogenous Retinal Detachment Due to Giant Retinal Tears.* Clinical Ophthalmology (Auckland, NZ), 2021. **15**: p. 1013.

37. Baba, T., et al., *Visual outcomes after surgery for primary rhegmatogenous retinal detachment in era of microincision vitrectomy: Japan-Retinal Detachment Registry Report IV.* British Journal of Ophthalmology, 2021. **105**(2): p. 227-232.

38. Ting, D.S., et al., *25-years Trends and Risk factors related to surgical outcomes of giant retinal tear-rhegmatogenous retinal detachments.* Scientific reports, 2020. **10**(1): p. 1-8.

Figures

Figure 1

Control normal eyes.

a. Horizontal b scan of a normal emmetropic eye automated with red and green segmentation lines, the red dots indicate the choriocapillaris flow. b. Horizontal b scan with red and green segmentation lines. c. Normal superficial vascular plexus (SVP) slab with the ETDRS-like sector grid overlay. d. SVP slab with a normal outlined foveal avascular zone (FAZ). e. Superficial perfusion indices and retinal thickness at different macular subregions. f. the color overlays on the OCTA angiography image indicate a normal vessel density value in the key to the right, and normal superficial vessel density (VD) perfusion indices are depicted above the image. g. Normal deep vascular plexus (DVP). h. Deep perfusion indices located at different macular subregions. i. The color overlays on the OCTA angiography indicate a normal VD value in the key to the right, and normal deep VD perfusion indices are depicted above the image. j. The image shows a normal choriocapillaris flow area. k. The image shows a normal FAZ area of 0.456 mm^2. I. The image shows a high definition (HD) 12 mm horizontal b scan of a normal myopic eye. m. The image shows a HD 12 mm horizontal b scan in a brighter color. n. Horizontal b scan with green and red segmentation lines, with red dots corresponding to the retina and choroidal vessels. o. Normal horizontal b scan with segmentation lines in a healthy myopic eye. p. A corresponding SVP slab. q. A normal DVP slab in a myopic eye. r. Normal perfusion indices with corresponding retinal thickness values at the different macula subregions. s. VD at SVP in a normal myopic eye, the color overlays on the OCTA angiography image indicate a normal vessel density value in the key to the left. t. and u. Images of the corresponding superficial and deep perfusion indices with different normal values as indicated above the images. v. The image depicts a normal choriocapillaris flow of 2.308 mm^2 at the selected subfoveal choriocapillaris area of 3.142 mm^2. w. The image depicts a normal, regular FAZ area of 0.561 mm^2.

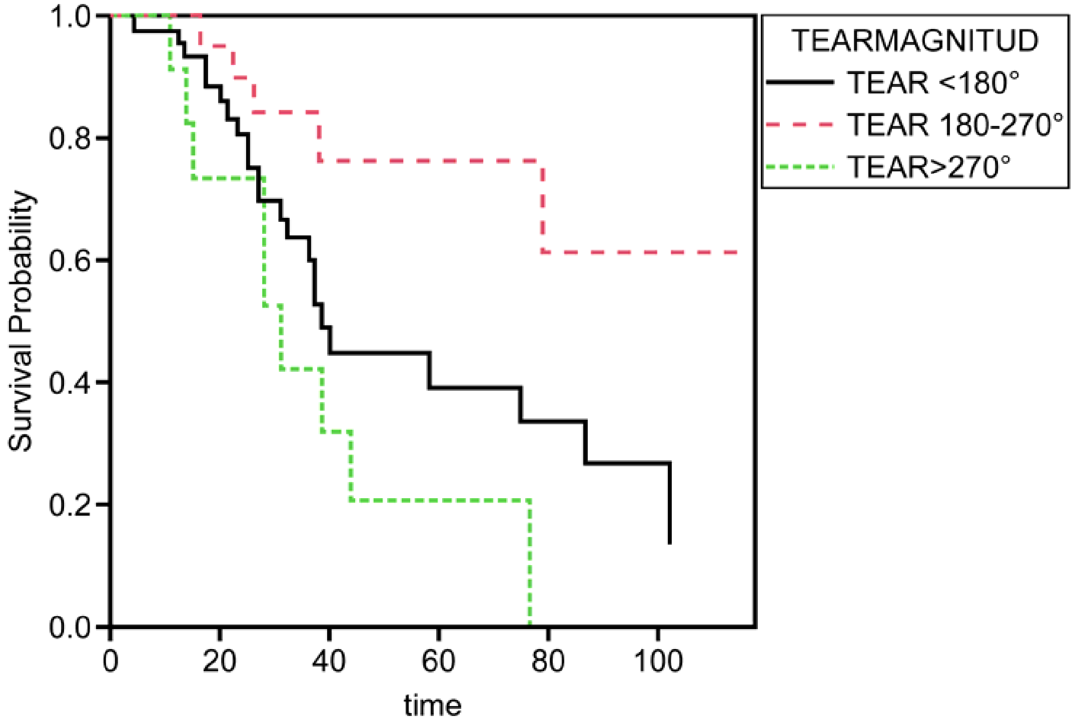

Figure 2

Kaplan–Meier survival plots. A Kaplan –Meier survival probability plot is included for tear magnitude. Each plot represents the survival probabilities of the different groups over time.

Figure 3

Surgical case 1.

a. Image of the fundus of a 55-year-old phakic, symptomatic woman presented with complaints of metamorphopsia and sudden visual loss in her right eye. The visual loss occurred over the period of seven days. The image showed a total retinal detachment due to a giant tear extending from the IX to I meridian. b. The image taken 6 weeks later shows a reattached retina with a well laser-sealed giant retinal tear. c. The image depicts postoperative HD 12 mm horizontal b scan. Several SD-OCT biomarkers were noted, such as an irregular foveal contour and internal and external neuroretina lines without total restoration of the central subfoveal ellipsoid zone and the external limiting membrane line. d. Superficial vascular plexus showing certain vascular deficiencies of the perfusion indices. e. Deep vascular plexus slab with better perfusion indices. f. Quantified superficial perfusion indices at different subregions of the macula. g. The color overlays on the OCTA angiography image indicate abnormal superficial VD value in the key to the left with the ETDRS-like sector grid overlay. h. The color overlays on the OCTA angiography image indicate a normal deep VD value in the key to the right. i. The image depicts deep perfusion indices at different subfields of the macula with the corresponding retinal thickness. j. Choriocapillaris flow area of 2.113 mm^2 at the selected subfoveal choriocapillaris area of 3.142 mm^2. k. Enlarged irregular non-flow tissue corresponding to a FAZ area of 4.036 mm^2.

Figure 4

Surgical case 2.

a. The image shows the fundus of a 52-year-old phakic, symptomatic myopic woman who presented with complaints of aggravating metamorphopsia and entopic phenomena, which were accompanied by a progressive and rapid drop in central vision. The right eye with an axial length of 26.38 mm and a macula-off giant retinal tear related rhegmatogenous retinal detachment of 200-degree extension over the temporal and superior quadrants underwent an uneventful gas-vitrectomy surgery. b. The image depicts the fundus at the 26-month follow-up; the operated eye showed a postoperative BCVA of 20/40 (logMAR 0.30). c. and d. Images depicting a high-definition SD-OCT horizontal b scan with an irregular foveal profile and diffuse retinal thinning; the outer retina biomarkers are identifiable. e. and f. The images show the corresponding superficial and deep vascular plexuses slabs. g. The image presents different values of the perfusion indices and retinal thickness at different subregions of the macula. h. and i. The images show the color overlays on the OCTA angiography images indicating superficial and deep vessel density values in the key to the right; the quantified perfusion indices in different subregions of the macula are depicted above.

Figure 5

Surgical case 3.

a. and b. The images show transoperative photos of a 39-year-old man with two days of sudden decrease in vision with metamorphopsia and high myopia. The patient was diagnosed with familial Stickler´s syndrome by the genetic unit. The diagnosis of a GRT-associated RRD of more than 270-degree extension was made. Counting fingers at 2 ft was assigned to a visual acuity of 20/2000 during preoperative BCVA (logMAR 2.00), with posterior staphyloma and an axial length of 30.10 mm. c. and d. Images after a 15-month follow-up showing an SD-OCT pattern consistent with an abnormal macular profile and the presence of abnormal biomarkers such as inner and irregular outer retina SD-OCT layers, abnormal subfoveal ellipsoid zone, and ELM line discontinuities with a well-preserved RPE layer. e. and f. The images depict superficial and deep vascular plexuses with the ETDRS-like sector grid overlay. g. and h. The images showing different perfusion indices values and corresponding retinal thickness at different subregions of the macula. i. and j. The images depict the color overlays in the OCTA angiography images indicative of superficial and deep vessel density values in the key to the right; the quantified perfusion indices on the different subregions of the macula are depicted above. k. The image shows a choriocapillaris flow area of 2.156 mm^2. l. The image depicts a highly abnormal, enlarged, irregular foveal avascular non-perfused area of 9.657 mm^2. m. The image depicts a long-term, postoperative central crossline b scan with an irregular foveal profile, internal limiting membrane remnants, external limiting membrane discontinuities and dissociated optic nerve fibers layers defects.